Seasonal Co-Variability of Surface Downwelling Longwave Radiation for the 1982-2009 Period in the Arctic

16th EMS Annual Meeting & 11th ECAC
12–16 September 2016 | Trieste, Italy

M. Boccolari [1], F. Parmiggiani [2]
[1]DSCG, University of Modena and Reggio Emilia, Modena (Italy)
[2]ISAC-CNR, Bologna (Italy)
Emails: mauro.boccolari@unimore.it; f.parmiggiani@isac.cnr.it

INTRODUCTION

The variability of sea ice extent in the Arctic is largely affected by changes in the surface downwelling longwave radiation [6], which is linked to cloudiness and which, in turn, depends on the atmospheric moisture transport to the Arctic. Aim of this work is to look for coupled spatial patterns in the Arctic of Surface Downwelling Longwave (SDL) and Sea Ice Concentration (SIC) fields, computed through the Maximum Covariance Analysis (MCA) technique. In addition, correlations between expansion coefficients time series of both variables and seasonal time series of AMO, AO, NAO, PDO and PNA indices are also presented. Data were retrieved from NSDIC and EUMETSAT. Instead of the standard seasons, the following ones were chosen: Feb-Mar-Apr (FMA), May-Jun-Jul (MJJ), Aug-Sep-Oct (ASO) and Nov-Dec-Jan (NDJ), as they are more appropriate for the Arctic climate.

1 DATA SETS

The following data sets were used:

- Arctic monthly sea-ice concentration (SIC) for the 1982-2009 period, distributed by the National Snow and Ice Data Center (NSIDC) [3]. SIC data are generated from brightness temperatures derived from SSMR, SSM/I and SSMIS observations. SIC data accuracy is generally ±5% of the total during winter, and ±15% during the Arctic summer melt and tends to be higher when sea ice is relatively thick (>20 cm). The spatial resolution, referred to a polar stereographic projection, is 25 x 25 km.

- Global monthly surface downward longwave radiation (SDL) for the 1982-2009 period. This is a subset of the global area cover (GCA) climate data set CLARA-A1 [7] produced by the EUMETSAT's Satellite Application Facility on Climate Monitoring (CM SAF). Data were generated from satellite-derived measurements of AVHRR sensor on-board of NOAA and Metop polar-orbiting meteorological satellites. In particular, SDL data are based on the monthly mean surface downwelling longwave radiation data from the ERA-Interim data set, on the CM SAF GAC cloud fraction (CFC) data set and on high-resolution topographic information. The resolution is 0.25° and the accuracy is 8 W/m^2 [4]. In this work, not all global data were used, but only those having latitude over 60°N. In addition, as we are interested to the Arctic Ocean co-variability, only SDL sea cells were considered, through a land/mask file computed by interpolating the equivalent NSDIC land/sea mask file with 12° resolution.

3 SEASONAL SPATIAL PATTERNS

The SVD technique was applied to seasonal SIC and SDL fields, after a proper sampling, for computational reasons, of the respective matrices. Thus, the size of each matrix submitted to the SVD was 21600 cells and 17024 cells for SDL (both sea and land) and SIC, respectively.

The fraction of squared covariance (SCF) (the SCF for i-th singular value ω_i is given by $\mathrm{SCF}_i = \omega_i / trace(\boldsymbol{\Omega})$) for the first five modes and for each season, is shown in Figure 1, together with the mean seasonal SIC in the 1982-2009 period. As can be noted, first two coupled patterns represent the 38%, 35%, 48% and 50% of the covariance.

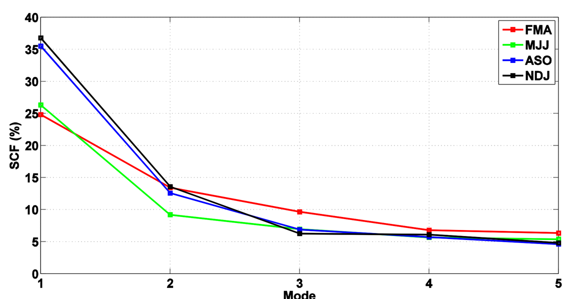

Figure 1. First five SCF values for each season.

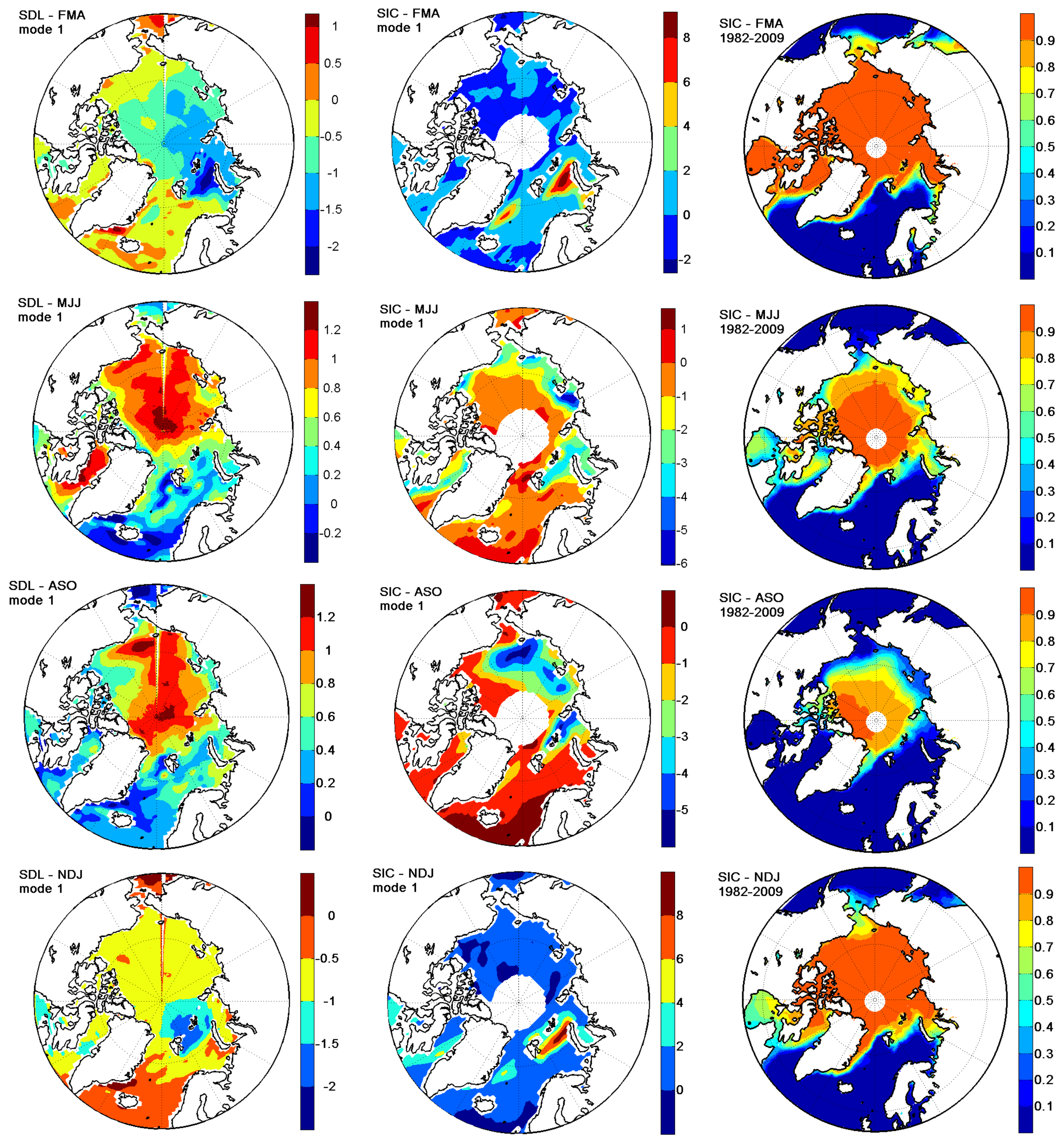

Figure 2. Seasonal spatial patterns (only 1st mode) of SDL (left) and SIC (middle), together seasonal SIC averages for the period 1982-2009 (right).

In Figure 2, the seasonal spatial patterns (first mode), together with the seasonal SIC means, for the 1982-2009 period, are shown. It can be noted that:

- SDL and SIC are out-of-phase: positive variations of SIC correspond to negative variations of SDL, and vice versa.
- During the "Arctic winter" (FMA), the maximum variability, both for SIC and SDL, is found in the Barents Sea. Similar patterns are observed in the standard winter (DJF).
- In the "Arctic spring" (MJJ), SDL maximum is located on the North Pole while SIC maximum in the Laptev Sea.
- During the "Arctic summer" (ASO), SDL maximums, found in the Chukchi Sea and in the North Pole, correspond to SIC maximum along Siberian coast from Chukchi Sea to Kara sea.
- Finally, in the "Arctic autumn" (NDJ) maximums are found north of the Barents Sea.

2 METHODS: Maximum Covariance Analysis

The Maximum Covariance Analysis (often incorrectly called Singular Value Decomposition analysis) is a technique that finds pairs of linear combinations, **U** and **V**, of two sets of vector data **X** and **Y** such that their covariances are maximized [13]. That is, if $\begin{cases}\mathbf{U} = \mathbf{L}^{\mathbf{T}}\mathbf{X} \\ \mathbf{V} = \mathbf{R}^{\mathbf{T}}\mathbf{Y}\end{cases}$ then $\mathbf{cov}(\mathbf{U},\mathbf{V}) = \mathbf{L}^{\mathbf{T}}\mathbf{S}_{\mathbf{X},\mathbf{Y}}\mathbf{R}$ is maximized with the constraint that L and R vectors are orthonormal. The vectors **L** and **R** are obtained through a singular value decomposition (SVD) of the cross-covariance matrix $\mathbf{S}_{\mathbf{XY}} = \mathbf{L}\,\boldsymbol{\Omega}\,\mathbf{R}^{\mathbf{T}}$ where $\boldsymbol{\Omega}$ is the diagonal matrix of singular values of SVD.

The method is usually applied in climatology to two combined data fields in order to identify pairs of coupled spatial patterns, with each pair explaining a fraction of the covariance between the two fields [2].

4 CORRELATION WITH CLIMATE OSCILLATION INDICES

Relevant modes of variability in the Arctic region can be: i) the Arctic Oscillation (AO) [12]; ii) the Pacific North America pattern (PNA) [1]; iii) the North Atlantic Oscillation (NAO) [5], even if NAO may be considered a particular case of AO; iv) the Pacific Decadal Oscillation [9] and the Atlantic Multidecadal Oscillation (AMO) [11] .

The correlation between these climate indices and the expansion coefficients provided from the SVD analysis for both seasonal SIC and SDL were estimated; Table 1 gives the statistically significant (at 95%) correlation coefficients of the first two main modes of co-variability.

Table 1 - Oscillation indices (OI) having correlation statistically significant at 95% with seasonal SDL (left) and SIC (right) till mode 2 of co-variability.

SDL			
Season	OI	Mode	Corr.
FMA	NAO	2	-0.46
	AMO	2	0.45
MJJ	NAO*	1	-0.39
	AMO	1	0.48
	AO	2	0.40
	AMO	2	-0.37
	NAO	2	0.47
ASO	PNA	1	0.54
	AO*	2	0.38
	AMO	2	-0.45
NDJ	PDO	1	0.41
	AMO	1	-0.63

SIC			
Season	OI	Mode	Corr.
FMA	PDO	1	0.48
	NAO*	2	-0.38
	AMO	2	0.54
MJJ	NAO	1	-0.44
	AMO	1	0.59
	AMO	2	-0.45
	AO	2	0.53
	NAO	2	0.53
ASO	PDO*	1	-0.39
	PNA	1	0.76
	AMO	1	0.57
	AO	2	0.48
	AMO	2	-0.57
NDJ	PDO	1	0.41
	AMO	1	-0.63

*the correlation is not statistically significant at 95% using a resampling method to calculate the correlation.

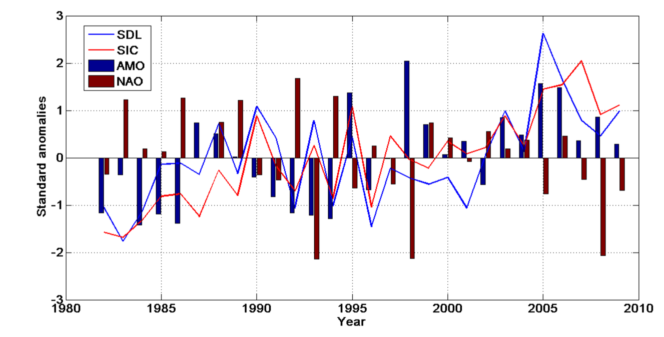

Figure 3. Vernal SDL and SIC expansion coefficients, for mode 1, together with NAO and AMO indices. All values were converted into standard anomalies.

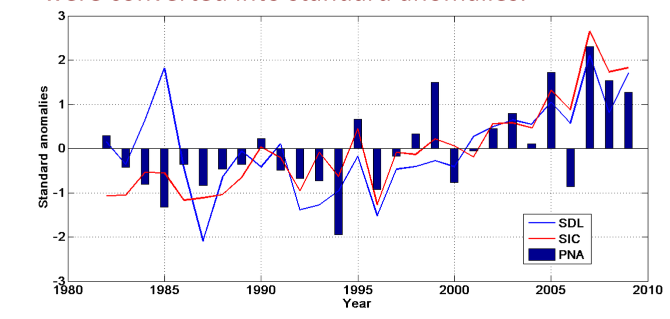

Figure 4. Summer SDL and SIC expansion coefficients, for mode 1, together NAO index. All values were converted in standard anomalies.

As can be seen in Table 1, expansion coefficients of the first mode of co-variability have statistically significant (at 95%) correlations with all envisaged climatic indices, in particular:

- The Atlantic Multidecadal Oscillation seems to be the climate oscillation that mostly affects both SIC and SDL during all seasons.
- On the other hand, the co-variability between sea-ice and AMO index is well-known [9]; this is particularly true in the Barents Sea during Arctic night months, with a correlation between the sea-ice and multidecadal variability [7].
- The strongest teleconnections which occur during FMA with NAO, PDO and AMO, are the same that can be seen in Dec-Feb months (not shown).
- Correlations with NAO and/or AO appear in all seasons, except in autumn, and are generally out-of-phase with AMO (Fig. 3 shows vernal NAO and AMO indices together with SDL and SIC expansion coefficients time series).
- PNA teleconnection is strong during melting season (ASO). Fig. 4 shows the summer index together with SDL and SIC expansion coefficients.
- Interesting to note from Fig. 4 the well-known sea-ice summer decline accompanied by the increase of SDL in the Arctic ocean.

CONCLUSION

This work shows where the Arctic spatial patterns of large co-variability between SIC and SDL (in out-of-phase) are located, in relation with the different season. For example, winter and summer strong patterns occur in the Barents Sea and the Chukchi Sea, respectively, in correspondence to one of two Atlantic gateways (the other is the Fram Strait) and in the Bering sea Pacific gateway. The more (less) moisture transport from these gateways implies a more (less) cloudiness and thus a more (less) SDL and, finally, a less (more) sea SIC (of course, this is just one aspect that affects the variability of the sea ice extension).

The contrast of the Atlantic/Pacific oceans is also enhanced by the analysis of the correlation between some natural oscillation indices and the time series of expansion coefficients of the first mode of co-variability: in winter, the correlation with AMO and NAO/AO seems to be prevalent but in summer the correlation with PNA becomes more important.

Finally, a shortcoming of this work is not having analyzed the cross-co-variability of SDL and SIC for different seasons, because it was demonstrated that SDL perturbations appearing during one season can alter the sea ice extent in the season ahead, for example, a disturbance of the SDL during spring may alter the sea ice extent in summer [6].

References

1. Barnston A. G. and R. E. Livezey (1987) Classification, seasonality and persistence of low-frequency atmospheric circulation patterns. Mon. Wea. Rev 115:1083-1126.
2. Bjornsson H. and S. A. Venegas (1997) A manual for EOF and SVD analyses of climate data. McGill University, CCGCR Report No. 97-1, Montréal, Québec, 52pp.
3. Cavalieri D. J. et al. (1996, updated yearly). Sea Ice Concentrations from Nimbus-7 SMMR and DMSP SSM/I-SSMIS Passive Microwave Data. Boulder, Colorado USA: NASA National Snow and Ice Data Center Distributed Active Archive Center. http://dx.doi.org/10.5067/8GQ8LZQVL0VL.
4. EUMETSAT Satellite Application Facility on Climate Monitoring (2012). CM SAF Cloud, Albedo, Radiation dataset, AVHRR-based, Edition 1 (CLARA-A1) Surface Radiation Products Algorithm Theoretical Basis Document. DOI: 10.5676/EUM_SAF_CM/CLARA_AVHRR/V001
5. Hurrel J. W. (1995) Decadal trends in the North Atlantic Oscillation: Regional temperature and precipitation. Science 269:676-679.
6. Kapsch M-L. et al. (2016) The effect of downwelling longwave and shortwave radiation on Arctic summer se ice. J. Climate, 29:1143-1159. DOI: 10.1175/JCLI-D-15-0238.1
7. Karlsson K.G. et al. (2013) CLARA-A1: a cloud, albedo, and radiation dataset from 28 yr of global AVHRR data, Atmos. Chem. Phys., 13:5351–5367.
8. Levitus S. et al. (2009) Barents Sea multidecadal variability. Geoph. Res. Lett., 36, L19604, doi:10.1029/2009GL039847.
9. Mantua N. J. et al. (1997) A Pacific interdecadal climate oscillation with impacts on salmon production. B Am Meteorol Soc 78:1069-1079.
10. Miles M. W. et al. (2014) A signal of persistent Atlantic multidecadal variability in Arctic sea ice, Geophys. Res. Lett., 41: 463–469, doi:10.1002/2013GL058084.
11. Schlesinger M.E. and N. Ramankutty (1994) An oscillation in the global climate system of period 65-70 years. Nature, 367, 6465: 723-726, DOI: 10.1038/367723a0.
12. Thompson D. W. J. and J. M. Wallace (1998) The Arctic Oscillation signature in the wintertime geopotential height and temperature fields. Geoph. Res. Lett., 5, 9:1297-1300.
13. Wilks D. S. (2011) Statistical methods in the atmospheric sciences. 3rd ed. Academic Press.

Acknowledgements

The authors are grateful to: National Snow and Ice Data Center (NSIDC) for the SIC data set; EUMETSAT for SDL products provided by the SAF on Climate Monitoring; Climate Prediction Center of the National Weather Service (USA) for providing monthly NAO and PNA indices; NOAA's National Centers for Environmental Information (USA) for providing the monthly AO index; NOAA's Earth System Research Laboratory (USA) for providing the monthly AMO index